Modeling and Dynamics of Tethered Formations for Space Interferometry

Marco Quadrelli♠

Abstract— **We describe a rather general model used to predict the dynamics and control performance of formations of spacecraft connected by tethers in heliocentric orbit and in low Earth orbit. The primary function of these systems is in Synthetic Aperture Radar and Space Interferometry aplications. Some numerical results demonstrate the applicability of these models.**

Keywords— **spacecraft, space interferometry, tethers, spacecraft control, dynamics, reconfiguration, baseline**

I. Introduction

Achieving the needed precision alignment, maneuvering, and synchronized motion of a set of spacecraft is a real challenge that we must face in the envisioned formation flying missions. Future Space and Earth Science missions involving space interferometers have been proposed which involve primarily three different types of spacecraft.

In the first type of space interferometer, a large, monolithic truss-based spacecraft supports the optical interferometric instrumentation and spacecraft bus within the same vehicle. The variable baseline of the interferometer is obtained by translating light collectors relative to one another along tracks to provide coarse baseline control, while fine control stages involving fast steering mirrors, voice coils, and piezoelectric stack remove residual errors and allow the system to reach the needed optical quality for the synthesized image. The need to have high resolution translates into the necessity of constructing a large track (10 meters in the Space Interferometer Mission), and therefore very large interferometers are precluded in this construction.

In the second type of space interferometers, separated spacecraft acting as light collectors and combiners fly in formation, and therefore very large baselines are possible. Examples of formation flying interferometric spacecraft are ST-3 (Space Technology 3) and TPF (Terrestrial Planet Finder). By accurately controlling the separation and relative angle between the individual spacecraft more or less autonomously, interferometric accuracies may be obtained for maintaining the instrument's baseline. The process of controlling the interferometer baseline usually occurs in two stages: a coarse control stage relies on on-board formation attitude control systems (by means of thrusters, reaction wheels) to drive the relative range and bearing to specified values, and a fine control stage relies on driving the optical elements on board the collector/combiner spacecraft (by means of variable delay lines using motor voice coils, piezoelectric stacks) to satisfy the more stringent optical metrology requirements. In this way, it is possible to reconfigure the entire formation configuration to a new baseline in the face of the enormous dynamic range imposed by kilometric distances and rapid dynamic changes.

In the third type of space interferometers, apertures of kilometric size are realized by connecting two or more light collecting spacecraft by means of one or more tethers. The advantage of using the tethers is that a variable controllable baseline can be achieved by reeling the tethers in or out, with a much smaller fuel consumption for reconfiguring the spacecraft compared to the case of separated spacecraft in formation, in which on-board thrusting is continuously required.

The presence of an extremely lightweight structural connection between spacecraft allows a degree of independence of the spacecraft, but at the same time constitutes a reconfigurable, large space structure capable of pointing and maneuvering as a unit. Depending of the envisioned application, different precision requirements exist: more stringent for space science applications such as interferometric observations or realization of large two-dimensional sensor arrays, less stringent for Earth science applications such as sensor webs responding effectively to events within the Earth system and for enabling human operation and exploration in space.

The idea of tethering the spacecraft to each other by means of a lightweight deployable tether is particularly attractive because: a variable baseline for interferometric observations can be achieved by deploying or retracting the tether [1]; the coverage of the observation plane can be done continuously by spinning the whole system; the high levels of propellant consumption currently demanded by the ACS (Attitude Control System) of separated spacecraft in formation can be dramatically reduced by clever tension control of the interconnecting tethers; two-dimensional and three-dimensional architectures can be constructed [2]. A gravitational wave detector based on connecting two masses via a tether has also been proposed in the literature [4], and tethered centrifuges for manned operations have also been studied ([9] and [10]).

Current approaches to formation flying envision separated spacecraft with sophisticated control architectures to enable control of the formation. However, none of the methods proposed to date are capable of dealing with system reconfiguration in a simple way [12]. The presence of an extremely lightweight structural connection between spacecraft allows a degree of independence of the spacecraft, but at the same time constitutes a reconfigurable, large space structure capable of pointing and maneuvering as a unit. Details of the synchronous deployment and

♠ Autonomy & Control Section, Jet Propulsion Laboratory, Pasadena, CA 91109

control strategy need to be investigated when more than two spacecraft are involved, as in two- or three-dimensional configurations.

An envisioned spacecraft operation scenario could be the following (in sequence of operations): the spacecraft reaches orbit; the spacecraft is pointed to a target; the vehicle is spun and at the same time the subsatellites are released; simultaneously, a counterrotating system of ballast masses is also deployed; at the end of deployment, the subbodies are located at the end of the tethers, which are kept stiff because of centrifugal forces. The whole spacecraft is now a zero-momentum spacecraft and can be three-axis stabilized around the target direction with thrusters or reaction wheels located in the central body without excessive power expenditure. Minor corrections which are needed for delay-line stabilization are taken care by tension control. Of course, the ACS capabilities have to be investigated, but in this configuration only the central body takes care of the ACS; three collectors are released from the hub, and they crawl up and down the tethers to cover the UV plane. Each collector needs only to be able to move up and down the radial lines and does not need to be a fully controlled sub-spacecraft by itself; while these collectors move, the moment of inertia of the system changes of some amount, but in a stable manner if these masses move synchronously, so that the whole system's attitude is also changing of some amount. This attitude change can be mitigated by moving slowly along the radial lines, and can be compensated by minor adjustments accomplished either by thrusters or by reaction wheels located on the central body. When the spacecraft needs to point to a different target, the crawler masses can be retracted to the hub, the total angular momentum is again exactly zero, and simple ACS from the thrusters/reaction wheels on the central spacecraft can reorient the whole system.

The work presented in this paper is in the direction of shedding light on the deployment/retraction and formation control characteristics of a planar and spatial assembly of more than two fully independent spacecraft connected by lightweight tethers to form a single monolithic spacecraft. In particular, this effort focuses on developing a computational modeling tool that includes: dynamics of tethers and subbodies in 2D and 3D configurations; environmental effects and perturbations, robust numerical integration capabilities. A set of control laws for formation stabilization and reconfiguration are analyzed. Studies are made on the impact of formation dynamics on pointing accuracy and, in the case of interferometric instruments, on baseline stabilization. Noise levels due to formation dynamics are estimated. Compensation of noise levels are also proposed.

The approach to be followed is based on a detailed finite element model of the tether and attitude dynamics of the sub-bodies. The basic environmental effects included in the model are the effect of solar pressure, gravitational perturbations, and thermal input that could cause the onset of thermal shocks. The philosophy behind the control scheme is that of allowing for spin-stabilized configurations, and precession of the spin angular momentum of the spacecraft in deep space by means of thrusters, tether deployment and retraction strategies based on tension control, and advantageous use of environmental forces (gravity, local magnetic field) to stabilize two-dimensional configurations in low planetary orbit.

The computational model is flexible enough to include: spacecraft in heliocentric orbit; with capability of controlling tether length and/or tension; with collectors capable of crawling along radial lines; with viscoelastic tethers (namely, with structural damping [6]); with environmental effects, including temperature changes [11], [3]. One goal is to demonstrate deployability, and to assess the feasibility of covering the interferometric UV plane with required precision when elasticity of the tethers (lag) is involved.

In short, we want to report on a simulation capability that will enable feasibility and dynamics/control prediction studies studies of different two-dimensional and three-dimensional tethered configurations; a set of control laws which will guarantee formation stabilization and formation reconfiguration for a class of tethered spacecraft lying on a plane or forming a large three-dimensional structure.

II. A Summary of Proposed Tethered Interferometer Aplications

The purpose of this section is to summarize some general facts about tether dynamics. Next, we will also review previous work appeared in the literature on Tethered Kilometric Interferometers (TKI), on Tethered Constellations (TCS) in LEO (electrodynamic-, drag-stabilized), on Spinning Tethered Systems in LEO (STS). One needs to be aware that there exists an extensive bibliography on concepts and applications [2]. Essentially, there exist two main motions for a space tether system: librational/spin and longitudinal/transverse oscillations. If Ω is the mean orbital motion, the in-plane librational frequency is approximately $\sqrt{3\Omega^2}$, whereas the out-of-plane librational frequency is approximately $\sqrt{4\Omega^2}$. The fundamental modes of motion are: bounce, transverse, longitudinal, skip-rope, end-mass coupling. The original concept for tether applications was a gravity-gradient stabilized (ULF antenna, plasma experiments) spacecraft in low Earth orbit. Other applications include spin-stabilized, electrodynamic waveguide, atmospheric probe. Because of the spatial extension, there exists a strong interaction with the environment. Thermoelastic dynamics (excited at terminator crossings) is very crucial due to thermal shocks on long line. Micrometeoroid hazard is a reality. Damping due to internal dissipation in a tether is effective only for longitudinal oscillations and useless for transverse ones. Structural damping for a kilometric tether is extremely difficult to predict, let alone to measure in flight. Active damping due to tension control is effective under a resonant tuning between the longitudinal and transverse oscillations. Both the tether tension (a function of the tether length, and length rate) and the tether length can be used as control variables for baseline stabilization. Tether tension/length control van be used to control in-plane and out-of-plane librations as well. Many control laws have been proposed in the literature to stabi-

lize oscillations and/or end-body attitude.Not many have been implemented. A controllable boom can be used to absorb tether energy over a wide frequency band, thereby mitigating the transfer of energy between the tether and the end spacecraft.

The Deployable Tethered Interferometer (TRIO) [1] proposal demonstrated that spinning tethered structures can be deployed to kilometric sizes providing a spiral path suitable for efficient aperture synthesis. Observation begins with arms retracted and no angular momentum on the system, with optical axis aligned to the target. An internal reaction wheel system is spun up. At steady state speed, telescopes are released. Six cables conenct each telescope to the hub, to provide attitude stability in relative angle to the hub reference frame. The scan of the UV Fourier plane is achieved in a spiral path. The advantages of this application are: a wide range of baseline lengths available via tethers; the baseline angle for a given baseline length varies through 360 deg, independently of the orbit; attitude changes are made with tethers retracted (the whole spacecraft collapsed as a rigid body); each tether can be gimbaled to each end spacecraft to uncouple attitude from tether dynamics; a composite tether may be used in the forma of a load bearing element (made of Kevlar), and a stress-free optical fiber used as data-channel. The disadvantages of this application were identified as: the cable experiences longitudinal and lateral oscillations difficult to damp; the system may be passively damped, but accurate baseline monitoring requires active damping. In any case, the central station requires an active attitude control system to provide inertial pointing.

One-dimensional, two-dimensional, and three-dimensional Tethered Constellations [7] are possible in space by imagining a set of spacecraft connected by tethers in multiple directions. Any generic distribution of more than 2 masses is space connected by tethers in a stable configuration is defined as a tethered constellation. Stabilizing forces can be a vertical gravity gradient, the differential air drag between the spacecraft in LEO (different ballistic coefficient), electrodynamic forces when the system is immersed in a magnetic field and currents flow along the tethers, and centrifugal forces arising from spinning the system. A combination of some of the above methods is also possible.

The Tethered Orbiting Interferometer (TOI) [8] was proposed as a RadioAstronomy Explorer satellite consisting of two end bodies joined by a flexible lightweight cable several kilometers long. The system was gravity-gradient stabilized with the long axis pointed towards Earth. Data on this configuration were collector masses (m1=75 Kg; m2=125 Kg); tether length L=5 Km; orbital period=10 hr; orbital eccentricity=0; semimajor axis=23560 Km. This system proved to have an increased secular orbital drift due to spacecraft flexibility: after one year of operation, coupling of gravitational and elastic energy yields an oscillatory perturbation of up to 138 m. This study points to the unexpected coupling between internal tethered spacecraft dynamics and the orbital dynamics.

Spinning Tethered Centrifuge in LEO ([9] and [10]) was a study carried out by the author on the dynamics and stability of a 1km-long orbiting centrifuge for artificial gravity applications. The essential features of the model used in this study are also used for ther simulation studies described below for tethetred formations. The main conclusions of this study were that: transverse oscillations are stable during spin; the controllability of acceleration-level on board the end bodies was demonstrated; and because of J2, the system's spin angular momentum vector precesses and drifts when spin axis is at 90deg to orbital plane, and precesses without drift when spin axis lies on orbital plane.

III. Model and Dynamics Analysis Needs for N spacecraft in tethered formation.

The fundamental points that need to be considered when thinking of modeling and dynamics analysis of low Earth orbit Formation Flying can be summarized as follows.

1) Environmental effects.

2) Multiple Dynamic Scales and Novel Formation Modeling Techniques.

A. Environmental Effects

Tethered spacecraft in heliocentric orbit are continuously subjected to solar pressure, hence the environmental model is quite benign given the low intensity of this perturbation (in any case, it needs to be counter-acted by the on board RCS). Instead, Low-Earth-orbit formations are subject to several non-uniform perturbations that can potentially destabilize the formation geometry. Atmospheric drag is predominant over all other effects up to an altitude of about 1000 kilometers. For large formations in low Earth orbit, the spacecraft at lower altitudes experience stronger retarding forces as compared to those at higher altitudes. Furthermore, the formation geometry is influenced by predominant perturbations induced by high Knudsen number flow at higher altitude. The effect of the atmospheric drag can be classified as a variable spatial perturbation on the formation that can only be accounted for by realizing the state coupling of the formation geometry. Therefore, a dynamic altitude density model for all altitudes must be included in the formation control model regardless of the type of mission for which the formation is designed.

The geomagnetic field has a non-negligible intensity in low Earth orbits. The field behaves as a disturbance source to the formation and introduces non-uniform perturbations to the formation geometry. This is particularly important if each spacecraft in the formation is carrying magnetic loops or is an element of a conductive circuit with the ionospheric plasma. The formation, in this case, acts as an electrical conductor, or equivalently, behaves as a cluster of dipoles that can be polarized in response to variations of the external gravitational and electromagnetic field. As a result, the variability of the external field that varies proportionally with the size of formation introduces variable differential forces and torques acting on different states of the formation. Thus a dynamic model of the geomagnetic field must

be incorporated in the formation control model to enable compensation for the effect of these perturbations.

Solar pressure is always present, but its effect is predominant above 1000 km. Solar pressure dictates an accurate radiation model of the spacecraft surfaces. The effect is analogous to Earth's albedo which acts on each spacecraft like a radiation pressure term at low altitude. Obscuration effects, implying a detailed shadowing analysis, become essential; hence solar pressure models are required in the formation control model when the formation requirements are tight.

Higher-order harmonics of the gravitational potential act as disturbance sources in large-scale spacecraft formations. In the case of micro- or nano-spacecraft formations, the effect is probably negligible on each individual spacecraft. For large-size spacecraft formations (fleets of membrane-like reflectors), however, the effect can impact the formation geometry since the formation can be viewed as distributed bodies with quasi-rigid shape and notable moment of inertia. The dynamic perturbation occurs at a frequency comparable with the orbital period, especially, when orbit changes are required. The formation states are then affected directly by different disturbances at frequencies corresponding to the various harmonics of the gravitational potential. A representative dynamic model of this phenomenon must be included in the formation control model to explore the impact on the formation geometry.

Finally, thermal input on each spacecraft from different sources such as: solar illumination, Earth's albedo, Earth's infrared radiation, and thermal output such as emitted radiation, needs to be taken into account for tight formation requirements. Although these effects may be negligible for micro- or nano-spacecraft, larger-size spacecraft are particularly sensitive to it in proportion to the exposed area. The inclusion of accurate environmental perturbations in the formation dynamic model, as well as, the formation control model is essential in all low types of Earth-orbit formations.

B. Multiple dynamic scales and novel formation modeling techniques for tethered-connected spacecraft.

A new scheme for representing the formation dynamics is presented that can analyze different classes of problems involving general orbiting formations. As a consequence, a rigorous framework will be available that will enable the analysis of general N-body formations, fleets, constellations, or collections of formations, in synchronous or asynchronous motion. We envision formations of different types: from a small number of moderate-sized spacecraft carrying deployable reflectors to hundredths or more microspacecraft with autonomous or semi-autonomous attitude, navigation, and control system on board, which are designed to map extensive domains of the geosphere, form communication networks, or act as distributed space warning and surveillance systems. These systems are capable of responding and altering their configuration in an autonomous manner to external stimuli such as, for instance, an increased solar activity or the requirement of more extensive Earth coverage upon request from ground. This is accomplished by reeling the tethers in or out in response to sensor data received at one or more collector spacecraft. This implies extremely flexible reconfiguration capabilities, as well as the ability of changing the topology of the graph representing the visibility of one spacecraft with respect to another.

The main motivation for addressing the modeling problem at different scales comes from a real need. We use the attribute global when referring to the formation as a whole, whereas we use the attribute local when referring to a single spacecraft only. A cluster of tethered spacecraft, with their own internal dynamics, which move in a cooperative fashion to accomplish a scientific goal, inevitably undergo both local dynamics (spacecraft reorientation, spacecraft reconfiguration) and global dynamics (formation reorientation, formation reconfiguration). An example is a formation of tether-connected membrane reflectors, in which significant membrane-type dynamics contributes at the local level while the fleet is undergoing a change of shape, and in which tether dynamics is dominant. Another example is a cluster of tethered microspacecraft which are designed to move synchronously, but in which sensor/actuator noise and disturbance sources originating at different locations in the formation cause deviations from the intended formation configuration and result in unexpected modes of deformation of the formation. As a consequence, very different time and space scales are simultaneously present in the dynamics. In addition, a precision-controlled tethered formation brings in the time scales of the sensor and actuators operating during reorientation and reconfiguration.

Each individual spacecraft is capable of changing its configuration in response to stimuli originated either from the exterior of the formation or within the formation itself. To have a picture in mind, one may think of the formation as a virtual truss in which the stiffness level of this imegined truss is dictated by the relative sensing/actuation precision of one spacecraft with respect to another. The tether dominates the low frequency motion of the virtual truss. Because of different relative visibility constraints between spacecraft within the tethered formation, the connectivity of this virtual truss can be quite general. Because of sensor/actuator noise and dynamic uncertainties, the model of this virtual truss is stochastic in nature. Therefore, one may identify that there exist at least two time scales, as well as at least two space scales, in the description of the dynamics of a formation. The spacecraft dynamics begins to emerge when a time scale of the stimuli internal or external to the formation is smaller than a time scale representative of the formation dynamics itself, whereas in the opposite case the formation behavior as a unit is predominant. Furthermore, these effects become more complicated and dramatically nonlinear when the formation undergoes large reconfigurations, both in relative translation and in attitude. From a mathematical standpoint, the presence of different time scales makes the initial value problem stiff in nature. This stiffness adds to the inherent numerical stiffness of the equations of tether dynamics. This implies

that new simulation techniques might be required when analyzing the motion and dynamics of dense and multiple formations. The issue of reconfiguring the formation brings into the picture the necessity of allowing for large motions, of commanding those motions, and of tracking them as well. The representation model becomes strongly nonlinear, with features typical of a multibody dynamical system held together by some sort of generalized joint.

The development and implementation of these crucial modeling issues will provide an invaluable tool capable of modeling any type of orbiting formation, and with the power of enabling command and control architectures of decentralized type which assume full autonomy of the constituent spacecraft.

IV. Model Description

In the following we describe some features of the model currently implemented in our simulation code. The final objective of our modeling effort is to provide a simulation environment with the following capabilities:

- 1. Orbital/Thermoelastodynamic analysis of a system of N spacecraft connected by one or more three-dimensional tethers.

2. Realistic orbital parameters representative of LEO or Heliocentric orbit.

3. A zooming orbital reference frame approach, in which the local dynamics of the tethered system is referenced to a point which tracks the reference orbital motion. This approach splits the dynamics in orbital with respect to inertial, and in local with respect to orbital.

4. Viscoelastic tether. Longitudinal oscillations controlled by damper tuned to 0.9 ratio.

5. Thermal tether dynamics.

6. Tether dynamics represented by a finite number of lumped masses capable of large displacements.

7. Variable tether length in each tether segment, commanded by varying the tether deployment and retraction rates at the end of each tether segment (assumes a point mass reel located on each spacecraft at the end of each tether).

8. Non-spherical gravity field (J0 and J2 harmonics of gravitational potential).

9. Thermal perturbations (Sun thermal/radiation input, Earth's infrared radiation, albedo). Cooling by emitted radiation only.

10. Dynamic atmospheric model (Jacchia 1977 model: diurnal variations linked to solar activity, seasonal-latitudinal variations, up to a height of 1000 km; nonrotating model).

11. Attitude dynamics of each spacecraft (no flexibility) with full actuation capabilities: Thruster-Based Reaction Control System and Reacton Wheel Based Pointing Control System.

12. Global Formation Commander representing a centralized controller which commands the position and attitude of each spacecraft within the formation to follow a specific reconfiguration pattern.

13. Each spacecraft is equipped with a sensor suite composed of IRU (Inertial reference Unit with accelerometers), Gyros, Star Tracker, AFF (Autonomous Formation Flying Sensor), and tether tension and length/length rate sensor.

14. A Tethered Formation Estimator located on-board each spacecraft which receives true dynamic sensor data and estimates real sensor data assuming user-defined sensor noise models.

15. Formation Controller, which drives the reconfiguration of the tethered spacecraft by varying the length of each tether segment in response to the inputs received from the Formation Commander.

Currently, we have concluded the verification of the features representing the open-loop dynamics part of our simulation environment. Implementation of the closed-loop features, namely, the development of the Tethered Formation Commander, Formation Controller, and Formation Estimator, and their integration with the open-loop dynamics module will be the subject of future work.

V. Numerical Results

The conceptual elements of the study program under consideration are shown in Figure 1. These elements are: a Formation Commander, a Formation Controller, a Formation Estimator, and a Formation Dynamics block. In this paper, we focus on the Formation Dynamics block only. The simulation is implemented in MATLAB/Simulink.A block diagram representing the simulation modules is depicted in Figure 2. Numerical results have been obtained in the open loop case for two different tethered system configurations currently envisioned as possible implementations of the concept for space interferometry applications: a three-spacecraft/two-tether system (upper left in Figure 3), and a four spacecraft/three-tether system (lower right in Figure 3). The tension in one of the tether segments as a function of time is shown in Figures 4 and 5. The very high frequency oscillations compared to the spin rate demand the use of a stiff integrator.

Figure 6 shows a model of a tethered Synthetic Aperture Radar Interferometer for LEO applications. Figure 7 and Figure 8 depict the in-plane and out-of-plane angle respectively, during approximately three orbits. The system orbits the Earth at 800 km altitude. Figure 9 shows the thermal stretch acting on the tether during the three orbits. These plots show some of the features of tether dynamics that our simulation is capable of handling.

VI. Conclusions

In this paper, we have reported the results of the initial phase of a study aimed at developing a Tethered Formation simulation environment. The models used for dynamics analysis and control are described. Preliminary numerical results obtained with our simulation capability are also presented for two Tethered Formation configurations currently envisioned as possible implementations of the concept for space interferometry applications: a three-spacecraft/two-tether system, and a four spacecraft/three-tether system. A future paper will report the developments of the Formation Commander, Formation Controller, and Formation Estimator whcih will make possible the analysis and im-

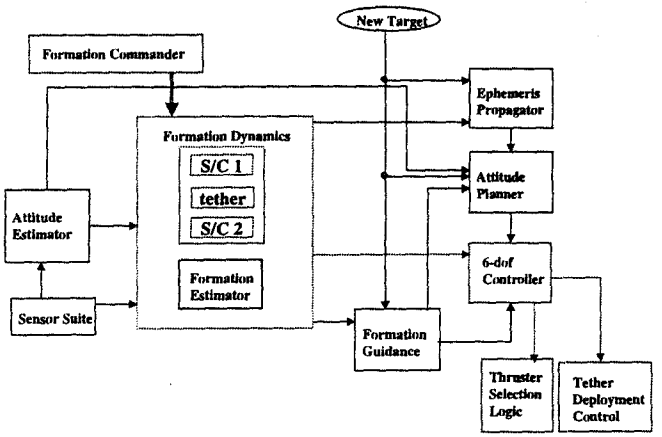

Fig. 1. Conceptual description of dynamics and control elements for Tethered Formation Flying Simulation.

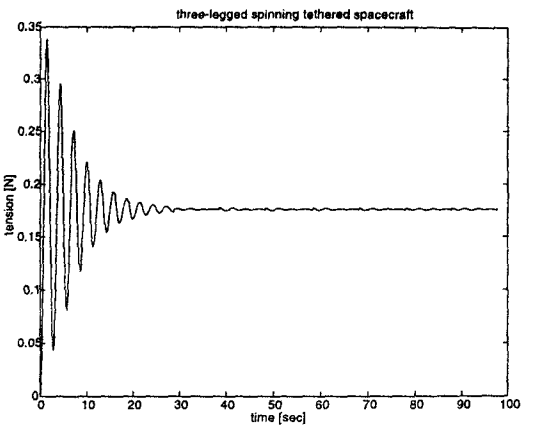

Fig. 4. Tether tension vs. time at stationkeeping for three-legged formation.

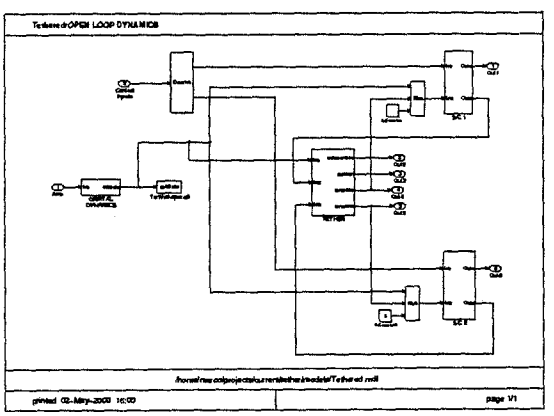

Fig. 2. MATLAB/Simulink block diagram showing simulation modules.

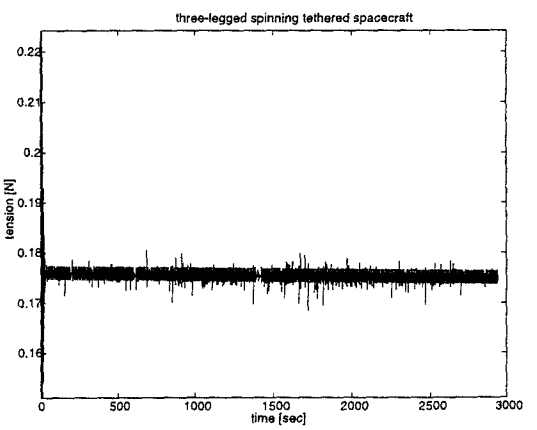

Fig. 5. Tether tension vs. time at stationkeeping for three-legged tethered formation.

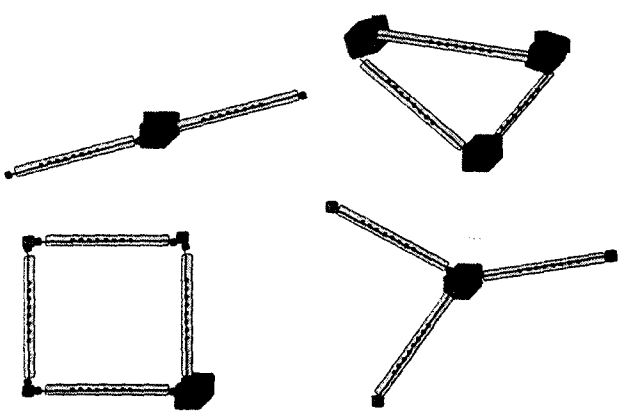

Fig. 3. Some of the Tethered Formation configurations currently being analyzed.

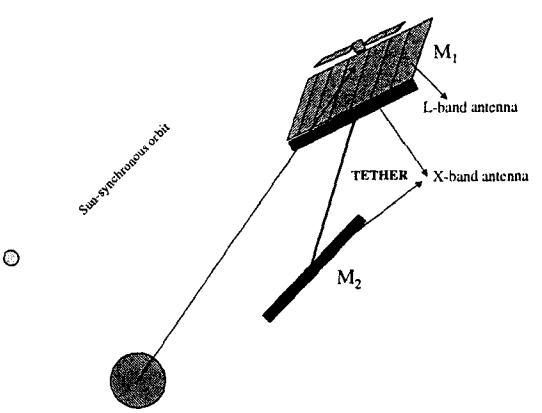

Fig. 6. A Tethered Synthetic Aperture Radar Interferometer in LEO.

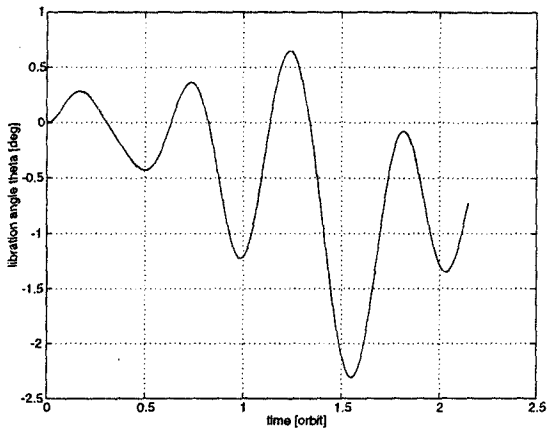

Fig. 7. In-plane angle for SAR interferometer.

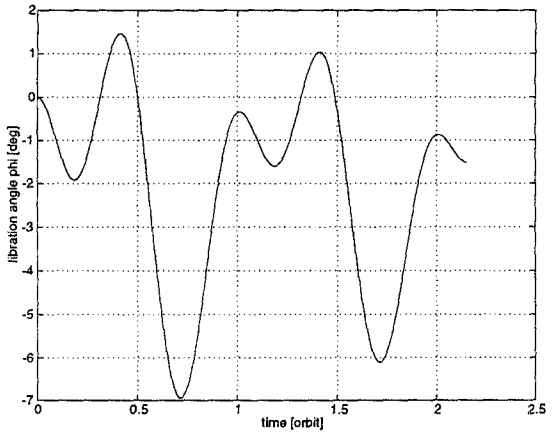

Fig. 8. Out-of-plane angle for SAR interferometer.

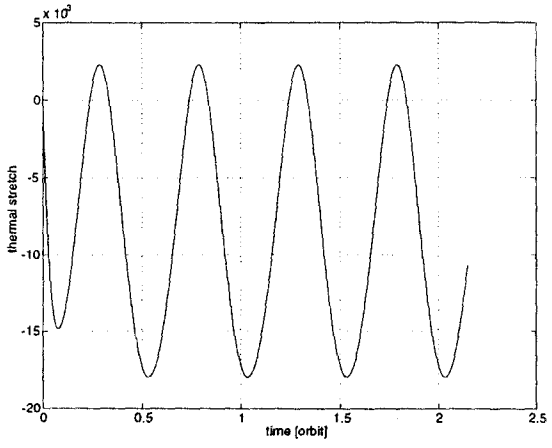

Fig. 9. Thermal stretch for SAR interferometer.

plementation of reconfiguration control schemes for very general configurations of Tethered Interferometers.

Acknowledgement 1: The author is very grateful to Dr. F. Hadaegh, Dr. G. Singh, Dr. J. Shields, Mr. A. Ahmed, Dr. E. Lorenzini, and Mr. G. Gullotta for helpful discussions. This research was supported by the NASA Distributed Spacecraft Thrust Area.

References

[1] Proceedings of the *Colloquium on Kilometric Optical Arrays in Space*, 23-25 October, 1984, Cargese, Corsica, France, European Space Agency.

[2] *Tethers in Space Handbook*, 2nd Edition, NASA Report NASW-4341, 1989.

[3] Beletskii, V.V. and Levin E.M.: *Dynamics of Space Tether Systems*, Advances of the Astronautical Sciences, vol. 83, 1993.

[4] Braginsky V.B., and Thorne, K.S.: *Skyhook Gravitational Wave Detectors*, Moscow State University and Caltech, 1985.

[5] Graziani F., Sgubini S., and Agneni A.: *Disturbance Propagation in Orbiting Tethers*, in Advances in the Astronautical Sciences, vol. 26, 1987, pp.301-315.

[6] He X. and Powell D.: *Tether Damping in Space*, Journal of Guidance, Control, and Dynamics, 1989.

[7] Lorenzini E.: *Novel Tether-connected Two-Dimensional Structures for Low Earth Orbits*, JAS, vol. 36, no. 4, Oct.-Dec. 1988.

[8] Misra, A.K. and Modi, V.J.: *The influence of satellite flexibility on orbital motion*, Celestial Mechanics, 17 (1978), pp.145-165.

[9] Quadrelli M. and Lorenzini E.: *Dynamics and Stability of a Tethered Centrifuge in Low Earth Orbit*, JAS. vol. 40, no. 1, Jan.-March 1992.

[10] Quadrelli, M.: *Attitude Dynamics of a Spinning Tethered System in LEO*, Dynamics of Flexible Structures in Space, Computational Mechanics Pub., Springer, 1990.

[11] Von Flotow, A. H. : *Some Approximations for the Dynamics of Spacecraft Tethers*, Journal of Guidance, Control, and Dynamics, vol. 11, no. 4, 1988, pp. 357-364.

[12] Wang, P.K.C., and Hadaegh, F.Y.: *Coordination and Control of Multiple Microspacecraft Moving in Formation*, Journal of the Astronautical Sciences, vol.44, no. 3, pp.315-355, Sept. 1996.

Modeling and Dynamics of Tethered Formations for Space Interferometry

Dr. Marco Quadrelli
JPL/Caltech, Pasadena, CA 91109-8099

February 13, 2001

Outline

1. Introduction
2. Assumptions of Model
3. Tether Dynamics
4. Controller/Commander
5. Sensing/Estimation
6. Simulation results
7. Conclusion

Acknowledgements

- Dr. F. Hadaegh, JPL, Dr. G. Singh, Dr. J. Shields, Mr. A. Ahmed, JPL

- Dr. E. Lorenzini, SAO

Model Description

1. Analysis of a system of N spacecraft connected by one or more three-dimensional tethers.

2. Orbital parameters representative of LEO or Heliocentric orbit.

3. A zooming orbital reference frame approach, in which the local dynamics of the tethered system is referenced to a point which tracks the reference orbital motion. This approach splits the dynamics in orbital with respect to inertial, and in local with respect to orbital.

4. Viscoelastic tether with thermal dynamics. Tether represented by a lumped masses approach.

5. Variable tether length, commanded by varying the tether deployment and retraction rates at the end of each tether segment (assumes a point mass reel located on each spacecraft at the end of each tether).

6. Comprehensive environmental model.

7. Attitude dynamics of each spacecraft (no structural flexibility is considered) with full actuation capabilities.

8. Global Formation Commander representing a centralized controller which commands the position and attitude of each spacecraft within the formation to follow a specific reconfiguration pattern. This reconfiguration is accomplished by varying the tether length and by spin modulation.

9. Each spacecraft is equipped with a sensor suite composed of IRU (Inertial reference Unit with accelerometers), Gyros, Star Tracker, AFF (Autonomous Formation Flying Sensor), and tether tension and length/length rate sensor.

10. A Tethered Formation Estimator located on-board each spacecraft which receives true dynamic sensor data and estimates real sensor data assuming user-defined sensor noise models.

11. Formation Controller, which drives the reconfiguration of the tethered spacecraft by varying the length of each tether segment in response to the inputs received from the Formation Commander.

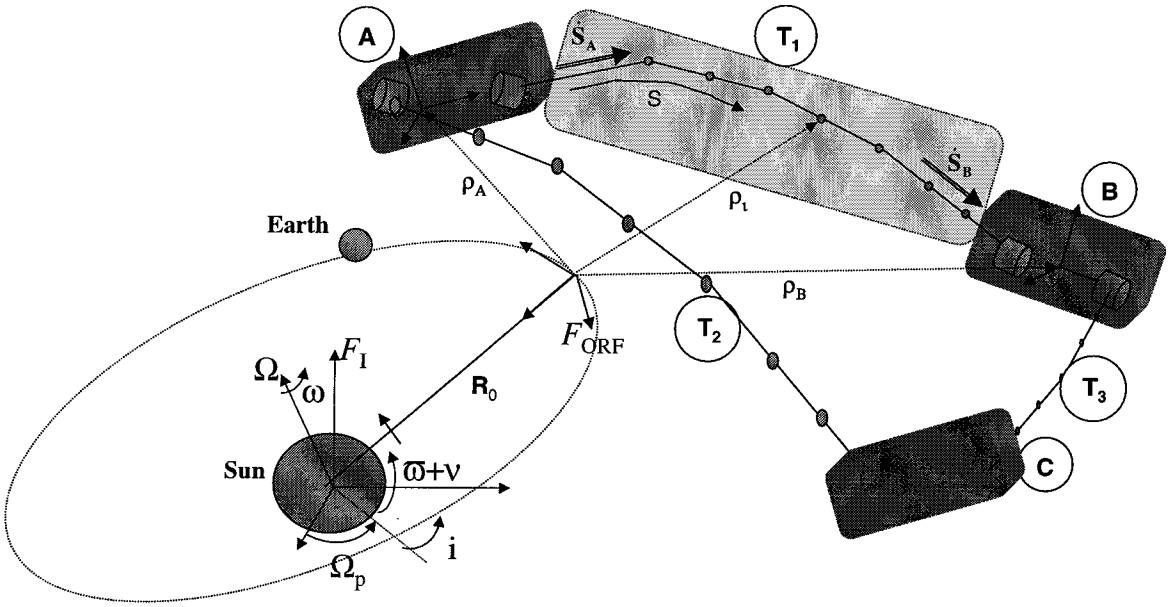

Geometric description of orbiting tethered formation.

Tether Kinematics and Kinetics

Our approach makes use of a material coordinate $\bar{s}$ which describes the arc-length of the tether in the undeformed configuration. Therefore, considering the tether segment T_i, connecting masses I and J, we have that at time t, $0 \leq \bar{s} \leq \bar{s}_I(t)$ defines the tether reeled in on the I-th spacecraft, $\bar{s}_J(t) \leq \bar{s} \leq l_{total}$ defines the tether reeled in on the J-th spacecraft, and $\bar{s}_I(t) \leq \bar{s} \leq \bar{s}_J(t)$ describes the deployed part of the tether. Clearly, $\bar{s}_I(t)$ and $\bar{s}_J(t)$ are prescribed functions of time representing the deployment and retrieval profiles, and we have that the currently deployed tether length is $\bar{l}(t) = \bar{s}_J(t) - \bar{s}_I(t)$. In $\mathcal{F}_{ORF}$, the position vector of a generic tether point is defined by $\rho(\bar{s}, t)$. Capital I and J denote the end masses, while lowercase i denotes tether points.

Operate a change of variables such that $\bar{s}(\xi, t) = \bar{s}_I(t) + \xi\, \bar{l}(t)$, so that $\rho(\bar{s}, t) = \rho(\bar{s}(\xi, t), t) = \tilde{r}(\xi, t)$. The tether element is defined by $\xi_i \leq \xi \leq$

ξ_{i+1}. Within this element, the average position $\rho_i(t) = \frac{1}{\triangle\xi}\int_{\xi_i}^{\xi_{i+1}} \tilde{r}(\xi,t)\,d\xi$ and the mass $m_i(t) = \mu\triangle\bar{s}$, where μ is the tether mass density, represent the position vector and mass of the lumped mass model. The kinematic equations of the interior tether points may be written as

$$\frac{d\boldsymbol{\rho}_i}{dt} = \mathbf{v}_i + G\left[\bar{l}, \frac{d\bar{s}_I}{dt}, \tilde{r}(\xi,t), \frac{d\bar{l}}{dt}, \xi_i, \xi_{i+1}\right] \tag{1}$$

while the dynamic equations may be written as

$$m_i\frac{d\mathbf{v}_i}{dt} = -\dot{m}_i\mathbf{v}_i + \mu H\left[\bar{s}_{i+1}, \rho(\bar{s}_{i+1},t), \bar{s}_i, \rho(\bar{s}_i,t)\right] + \mathbf{f}_i^{ext} + \mathbf{f}_i^{gyro} + \tau_{i+1} - \tau_i \tag{2}$$

where G and H are functions of the geometry of adjacent nodal points in the finite difference scheme. This is a finite difference approximation of the tether partial differential equation. As such, the large angle tether dynamics is correctly captured, and the approximation improves with the number of tether mass points.

The end body kinematic equations are

$$\frac{d\boldsymbol{\rho}_I}{dt} = \mathbf{v}_I \tag{3}$$

$$\frac{d\mathbf{q}_I}{dt} = \frac{1}{2}\langle \bar{\omega}_I \rangle \, \mathbf{q}_I \tag{4}$$

where $\bar{\omega} = \begin{bmatrix} \omega^T & 0 \end{bmatrix}^T$, and $\langle \cdot \rangle$ performs the quaternion multiplication.

The dynamic equations for the I-th spacecraft at the end of one tether segment are

$$m_I \frac{d\mathbf{v}_I}{dt} = \boldsymbol{\tau}_I + \mathbf{f}_I^{momentum\_flux} + \mathbf{f}_I^{gyro} + \mathbf{f}_I^{ext} \tag{5}$$

$$\mathbb{J}_I \dot{\omega}_I + \omega_I \times (\mathbb{J}_I \omega_I + \mathbf{h}_I) = \mathbf{g}_I^{ext} + \mathbf{g}_I^{rw} + \mathbf{g}_I^{tension} + \mathbf{g}_I^{momentum\_flux} \tag{6}$$

$$\dot{\mathbf{h}}_I = -\mathbf{g}_I^{rw} \tag{7}$$

where $\mathbb{J}_I$ is the moment of inertia matrix of the I-th spacecraft, $\mathbf{h}_I$ represents the total internal angular momentum distribution present in the I-th body (from reaction wheels). Notice the presence of convective terms also in the end mass linear and angular momentum balance equations. They represent the contribution of the momentum flux at the tether feedout point.

Finally, the tether thermal equilibrium is described by the first order differential equation

$$\dot{\vartheta} = \frac{Q^{incident} - Q^{emitted}}{\rho c m} \tag{8}$$

where ϑ is the tether temperature, $Q^{[\cdot]}$ represents a heat flux, r is the tether radius, ρ is the tether volume density, c is the tether heat capacity, and m is the tether mass.

Following [Quadrelli & Lorenzini,1992], since the spring mass frequency is too low for the natural material damping to be effective, a longitudinal damper is added in series to the tether itself at one of the tether attachment points. This is a passive damper, tuned to the frequency of the tether bounce mode. An additional dynamic equation is present, representing the linear momentum balance of the tuned damper as

$$k_t l_t = k_d l_d + c_d \dot{l}_d \tag{9}$$

The total tether strain and strain rate for the tether segment of length $l_{\Delta\xi}$ are

$$\varepsilon_{\Delta\xi} = \frac{l_{\Delta\xi}}{\bar{l}} - 1 \tag{10}$$

$$\dot{\varepsilon}_{\Delta\xi} = \frac{\bar{l}\frac{dl_{\Delta\xi}}{dt} - l_{\Delta\xi}\frac{d\bar{l}}{dt}}{\left(\bar{l}\right)^2} \tag{11}$$

so that the tether tension in the tether segment of length $l_{\Delta\xi}$, stiffness coefficient k and damping coefficient c, is

$$\tau_{\Delta\xi} = k\varepsilon_{\Delta\xi} + c\dot{\varepsilon}_{\Delta\xi} \tag{12}$$

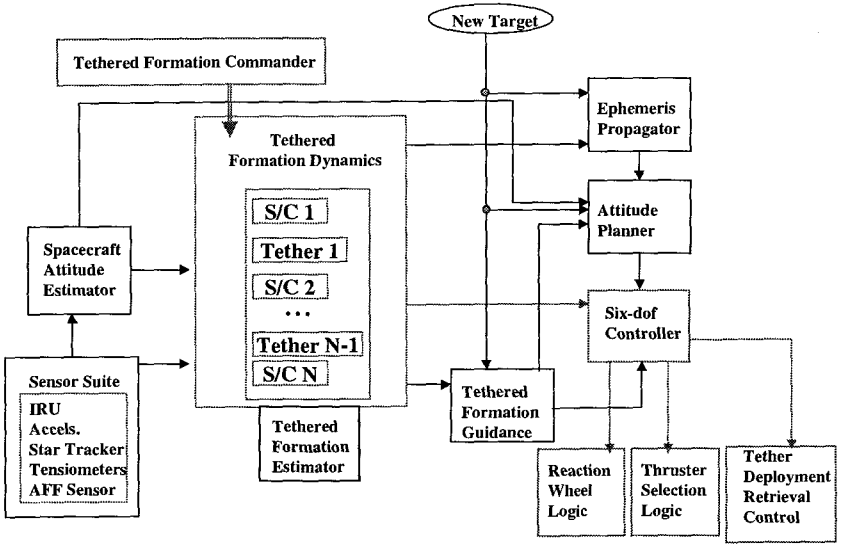

Conceptual description of dynamics and control elements for Tethered Formation Flying Simulation.

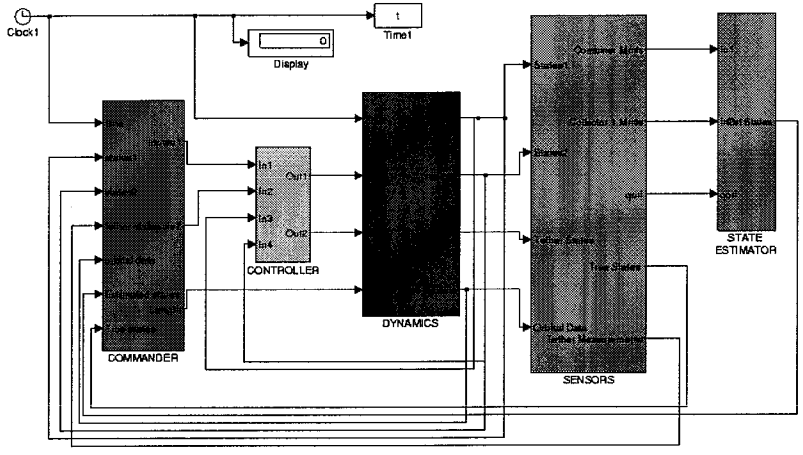

Simulink System Block Diagram.

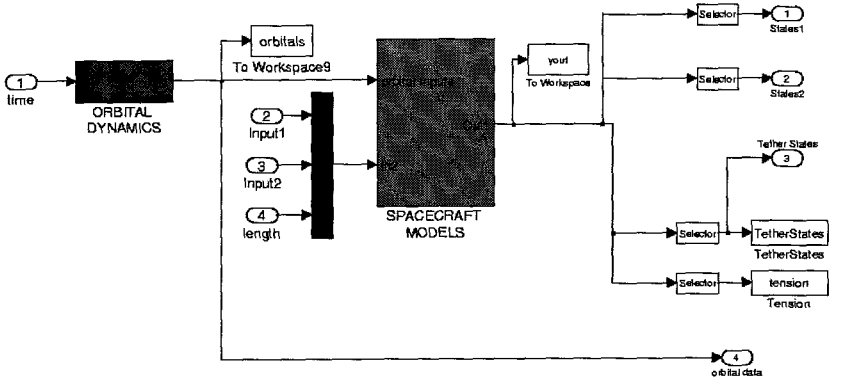

Dynamics Block.

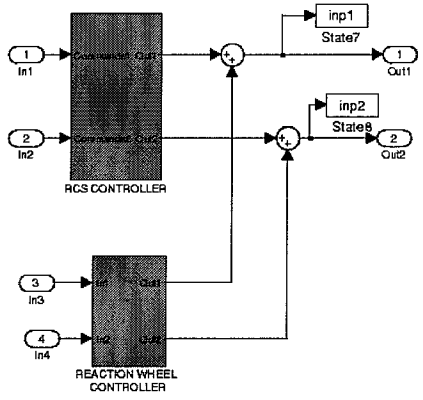

Control Block.

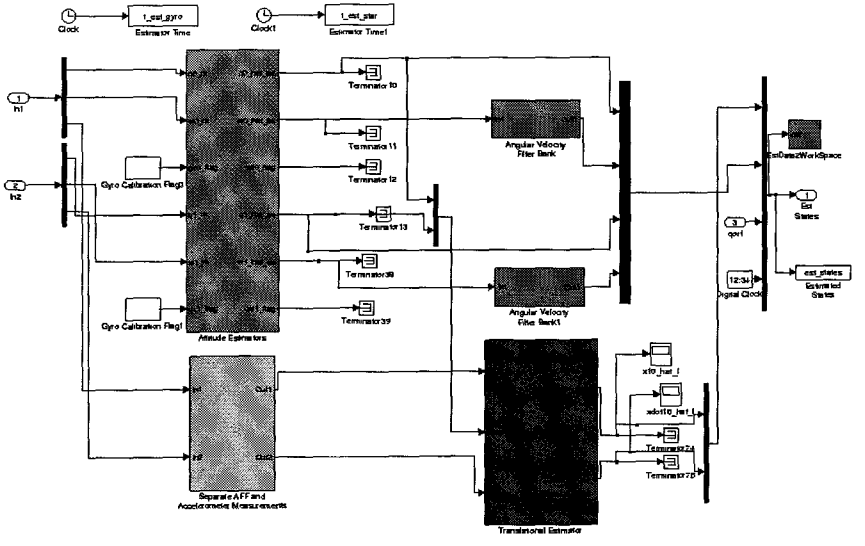

Estimator Block.

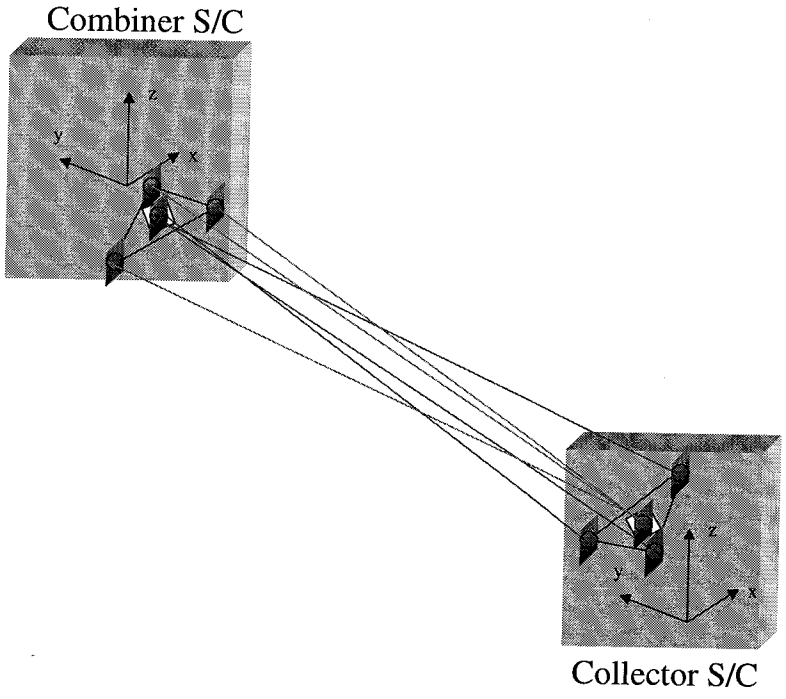

Autonomous Formation Flying Sensor. One transmitter and three receiver units on board each spacecraft.

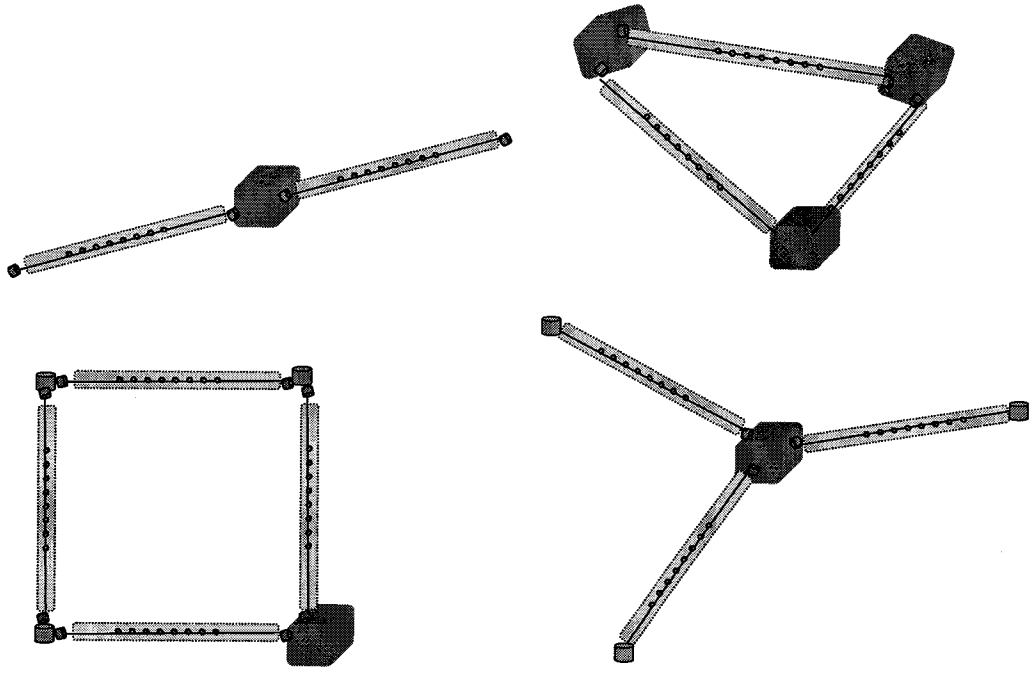

Some of the Tethered Formation configurations currently being analyzed.

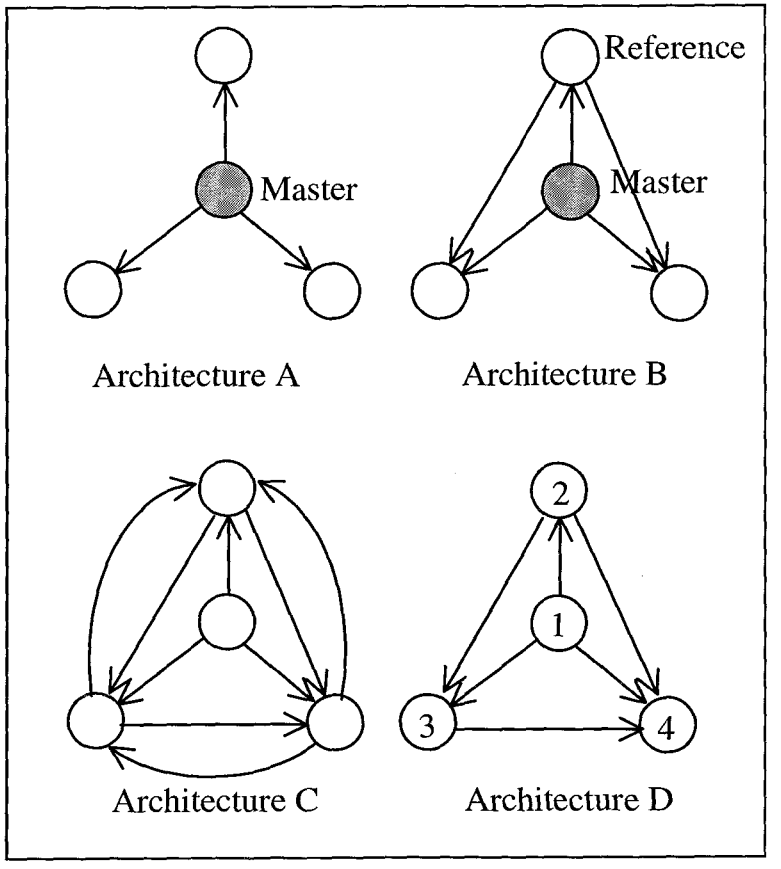

Four possibilities of making relative state measurements.

Sensing/Estimator

After measurement and estimation, the following input data is available to the Commander/Controller. For each spacecraft, we have: linear position, velocity, acceleration vectors in $\mathcal{F}_{ORF}$ with respect to O_{ORF}; quaternion, angular velocity, angular acceleration vectors in $\mathcal{F}_I$; relative bearing and bearing rate, relative range and range rate. Available variables at each tether feedout point are: tether length, length rate, length acceleration, tether tension, tether material strain and strain rate (thermal and mechanical). Available spin variables are: in-plane angle and rate, out-of-plane angle and rate, and current orientation of spin plane in $\mathcal{F}_{ORF}$ and $\mathcal{F}_I$.

Commander/Controller

The actuator mechanisms present on board each spacecraft are a Proportional Thruster-Based Reaction Control System and a Reaction Wheel Based Pointing Control System. The proportional thrusters are of three different types: coarse, fine, super-fine. The coarse RCS is used for retargeting and spin modulation. The fine RCS is used for attitude maneuvering and wheel desaturation, and the super-fine RCS is used for baseline modulation. The reaction wheel dynamic model contains viscous drag torque, ripple torque, and back emf motor torque. In addition, the reaction wheels are a source of noise, as it is assumed that wheel-specific imbalance forces and torques (modeled as wheel-rate dependent time series) act at the mounting location. This imbalance model type is empirical, where wheel disturbances consist of discrete harmonics of reaction wheel speed with amplitudes proportional to square of wheel speed.

We only consider the dynamics of the collector(s) relative to the combiner. We call this regime *internal* dynamics, which is different that the *external* dynamics mode in which the whole spacecraft receives commands aimed at changing its orbital dynamics (navigation-dependent mode). There are at least four internal dynamics control modes in the system working as an interferometer. The figure represents one level of uv-plane coverage named *full 2-D coverage* for the DS3 (two collectors, one combiner, two spacecraft) spacecraft. The solid line represents the uv-plane coverage at one epoch. The dashed line represents observations three months after the initial epoch (when the Sun-source angle has changed). Measurements of the target source are made every 100 meters along each track. We may classify them depending on their resulting dynamic response and relationship to the various phases of the observation cycle. The observation cycle is at least of two types: *Stop and Stare* observing mode (in which the configuration is brought to a halt with zero relative velocity between spacecraft before any observations are attempted), *Observe on the*

Fly mode (in which fringe measurements on astronomical targets can be made while the spacecraft are moving).

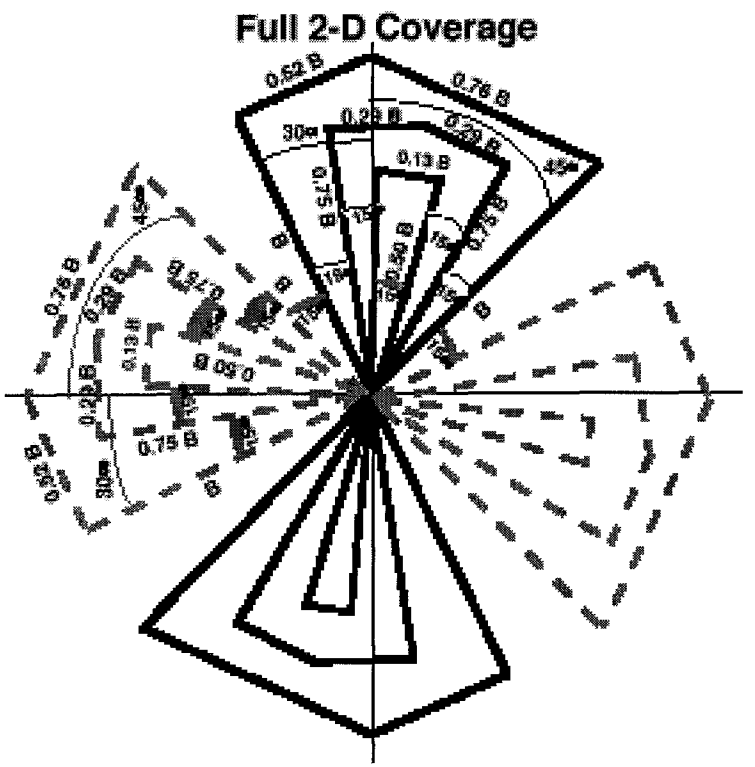

Full 2-D coverage (from an Internal JPL Document).

Attitude Rigidity Control Mode. This mode is used for fine pointing and stabilization only. It uses the Reaction Wheel Assembly located on each spacecraft, and uses local attitude and angular rate measurements on board each spacecraft, as well as information from the relative Attitude Estimator to ensure that bearing and bearing rate is within the specifications of the interferometer instrument (arcminute level or less). In general, the commanded torque vector on the reaction wheels of the i-th spacecraft aligning itself with the j-th spacecraft will be of the quaternion-feedback type:

$$\tau_i = -Pq_{ij} - D\omega_{ij} \tag{13}$$

where q_{ij} is the relative quaternion, and P and D are controller gains.

Spin/Despin Control Mode. This mode is used to modulate the rotational spin rate of the system about its center of mass. This mode involves coarse level thrusters (20N level or above) firing tangentially (orthogonal to the spin vector) and depends on a precise estimate of the in-plane and out-of-plane angles between the line connecting two end spacecraft and the spin plane (global attitude measurements). For spin or despin to a new rate ω_{new}, we use thruster forces in the spin plane (they will have to be converted to body axes and distributed among the existing thrusters) of the proportional-derivative form :

$$F = -\frac{K}{l_b}\left[(\theta - \omega_{new}t) + \tilde{\tau}\dot{\theta}\right] \tag{14}$$

where $\tilde{\tau}$ is a controller (settling) time constant, and l_b is the current baseline length.

Tether Deployment/Retrieval Control Mode. This mode is used to change the baseline of the interferometer (in which case this is a coarse actuation device), or to fine control the baseline for corrections at the centimeter level or less. This mode involves a continuous operation of the tether reels and fine thrusters (0.9N to milliN level), and a reliable operation of the Autonomous Formation Flying Estimator (for range and range-rate measurements) and Attitude Estimator on board each spacecraft. Given the length profile as a function of time $l = l(t)$, as specified by the instrument observation profile, the reel dynamics equations are inverted to obtain the commanding torque from the coupled equations of a variable inertia electric motor:

$$\begin{aligned} \tau_c &= \tau_c\left(l,\, \dot{l},\, \ddot{l}\right) \\ &= J_{reel}\ddot{\alpha} + \dot{J}_{reel}\dot{\alpha} - Tr\left(l\right) \end{aligned} \tag{15}$$

$$V_a = K_v\dot{\alpha} + \frac{R}{K_i}\tau_c\left(l,\, \dot{l},\, \ddot{l}\right) \tag{16}$$

where K_v, R, and K_i are electric motor constants, α is the drum angle, T is the tether tension, r_0 and $r(l)$ are initial and current drum radius (which is a function of the tether length deployed, and is usually obtained from controlled measurements during careful winding of the drum), h is the drum length, ρ_t is the tether material density, and J_0 and $J_{reel} = J_0 + \frac{\pi \rho_t h}{2}\left[r^4(l) - r_0^4\right]$ are the initial and current moment of inertia of the motor armature and drum.

Retargeting Mode. This mode is used when the tethers are retracted into the collector spacecraft, and the whole system is repointed to a different target before the whole sequence of u-v plane coverage begins for the new target. This mode involves a precession maneuver, which is accomplished by firing the external (coarse) thrusters of the collapsed spacecraft assembly and relies on precise attitude knowledge only. In general, the commanded torque vector on the RCS of the collapsed spacecraft retargeting from the current q to the desired q_{des} will be of the quaternion-feedback type:

$$\tau_i = -P_{rt} q_{error} - D_{rt} \omega_{error} \tag{17}$$

where q_{error} and ω_{error} are the quaternion error and angular rate, and P_{rt} and D_{rt} are controller gains which depend on the inertia of the collapsed spacecraft (i.e. at zero tether length).

Environmental Models

1. Non-spherical gravity field (J0 and J2 harmonics).

2. Thermal perturbations (Sun thermal input, Earths infrared radiation, albedo). Cooling by emitted radiation only.

3. Dynamic atmospheric model (Jacchia 1977 model: diurnal variations linked to solar activity, seasonal-latitudinal variations, up to a height of 1000 km; nonrotating model).

Numerical Results

Examples considered:

- Three tether, four spacecraft configuration
- Two spacecraft, one tether configuration
- Tether length: 1000m; spinrate=0.01 rpm; sinusoidal deployment and retrieval profile;

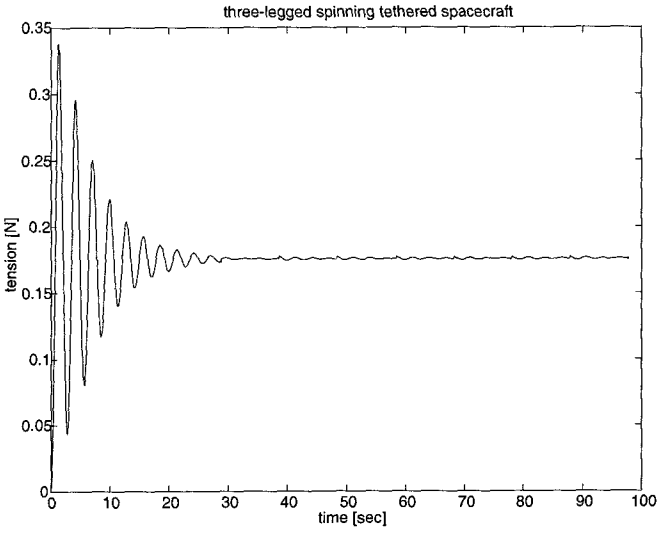

Tether tension vs. time at stationkeeping for three-legged formation.

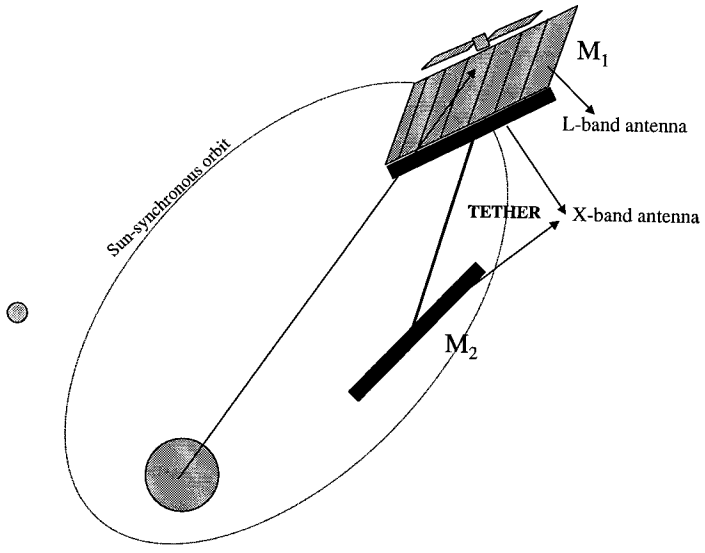

Model of an Orbiting Tethered Synthetic Aperture Radar.

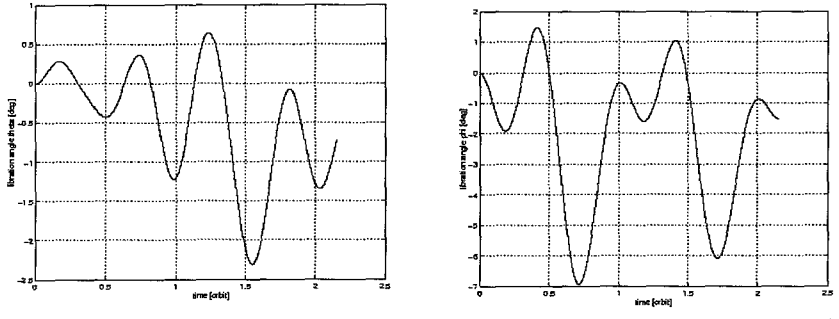

In-plane (left) and out-of-plane angles (deg) for Tethered SAR Interferometer during approx. three orbits.

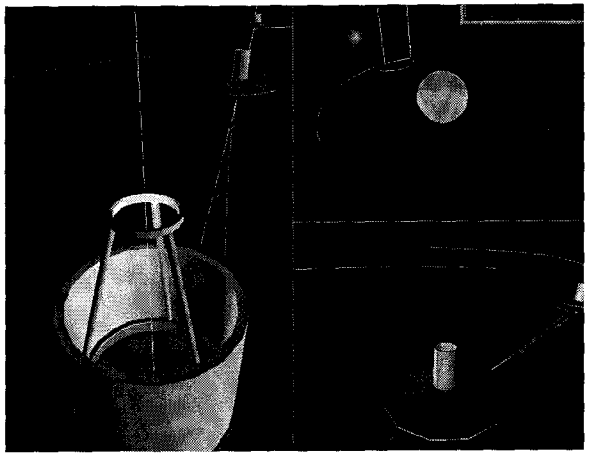

Snapshot of animation of tethered interferometer in heliocentric orbit.

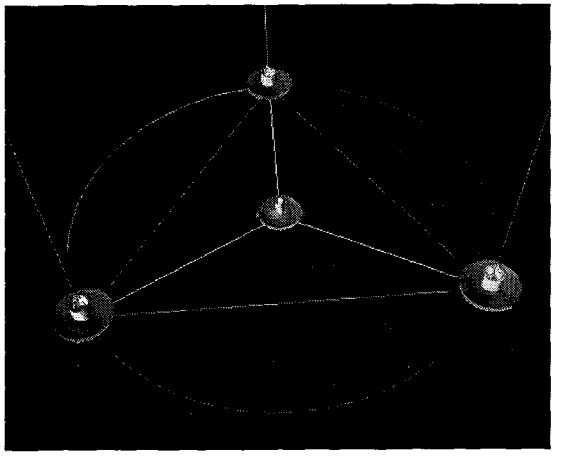

Snapshot of animation of three-legged tethered interferometer in heliocentric orbit.

Conclusions

1. Described a general simulation tool for tethered formations applicable to LEO and Heliocentric scenarios

2. Tether Dynamics couples variable-length with attitude dynamics in general topologies

3. Controller/Commander performs in 4 modes

4. Sensing/Estimation introduces AFF sensor for relative range and bearing

5. Simulation results presented for LEO and deep space applications

6. Future work: robust controllers, optimal reconfiguration maneuvers, moving attachment point, tether crawler.